GlucoLens: Explainable Postprandial Blood Glucose Prediction from Diet and Physical Activity
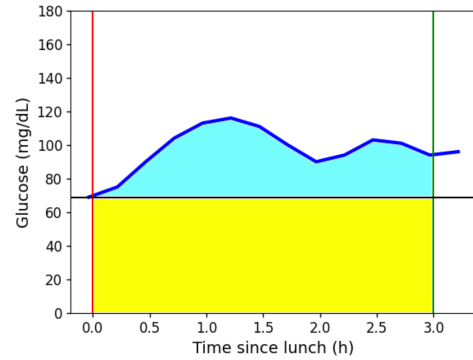
Abdullah Mamun[1,2,*], Asiful Arefeen[2], Susan B. Racette[2], Dorothy D. Sears[2], Corrie M. Whisner[2]
Matthew P. Buman[2], Hassan Ghasemzadeh[2]

Abstract—Postprandial hyperglycemia, marked by the blood glucose level exceeding the normal range after meals, is a critical indicator of progression toward type 2 diabetes in prediabetic and healthy individuals. A key metric for understanding blood glucose dynamics after eating is the postprandial area under the curve (PAUC). Predicting PAUC in advance based on a person's diet and activity level and explaining what affects postprandial blood glucose could allow an individual to adjust their lifestyle accordingly to maintain normal glucose levels. In this paper, we propose *GlucoLens*, an explainable machine learning approach to predict PAUC and hyperglycemia from diet, activity, and recent glucose patterns. We conducted a five-week user study with 10 full-time working individuals to develop and evaluate the computational model. Our machine learning model takes multimodal data including fasting glucose, recent glucose, recent activity, and macronutrient amounts, and provides an interpretable prediction of the postprandial glucose pattern. Our extensive analyses of the collected data revealed that the trained model achieves a normalized root mean squared error (NRMSE) of 0.123. On average, GlucoLense with a Random Forest backbone provides a 16% better result than the baseline models. Additionally, GlucoLens predicts hyperglycemia with an accuracy of 74% and recommends different options to help avoid hyperglycemia through diverse counterfactual explanations. Code available: https://github.com/ab9mamun/GlucoLens.

Index Terms—machine learning, metabolic health, continuous glucose monitoring, diabetes, hyperglycemia

I. INTRODUCTION

Hyperglycemia, or high blood sugar, occurs when the body cannot effectively regulate glucose levels. Hyperglycemia is defined as having a blood glucose (BG) level above 140 mg/dL [1]. Lack of physical activity and overconsumption of carbohydrates can affect a person's metabolism and affect the ability to regulate glucose [2]. People with untreated hyperglycemia are at increased risk of developing complications such as eye problems (retinopathy), kidney problems (nephropathy), nerve damage (neuropathy), heart disease, stroke, poor blood flow to the limbs, and are also more likely to experience depression [3]. While hyperglycemia can

[1]School of Computing and Augmented Intelligence, Arizona State University, Phoenix, AZ 85054.

[2]College of Health Solutions, Arizona State University, Phoenix, AZ 85054.

[*]Corresponding author.

Emails: {a.mamun, aarefeen, susan.racette, dorothy.sears, cwhisner, mbuman, hassan.ghasemzadeh}@asu.edu.

Fig. 1: An example of calculation of Postprandial Area Under the Curve (PAUC), Increase in PAUC from the projected area after lunch (ΔPAUC), and Maximum Postprandial Blood Glucose (MaxPBG).

affect anyone, individuals with prediabetes or diabetes are at a higher risk compared to healthy people [4], [5].

The Centers for Disease Control (CDC) estimates that 38% of American adults are prediabetic and almost 20% of them are unaware of their condition [6]. To help prevent the increasing prevalence of hyperglycemia and prediabetes, the Food and Drug Administration (FDA) has approved the sale of Continuous Glucose Monitors (CGMs) over the counter in the U.S. in 2024, making them more accessible to people with or without diabetes [7]. Prediabetes can be reversed with proper lifestyle management, such as diet and physical activity [8]. However, if left untreated, it can develop type 2 diabetes, which is an irreversible lifelong condition [9].

Healthy individuals are expected to maintain their BG between 60 mg/dL and 140 mg/dL, but it is not uncommon for them to have BG over the recommended range for a short duration after eating certain meals. The area under the BG curve for a certain duration (e.g., 2 or 3 hours) after a meal is known as the Postprandial Area Under the Curve (PAUC). An example of calculating PAUC, change in PAUC, and the maximum postprandial blood glucose (MaxPBG) is shown

in Fig. 1. The value of the PAUC is an important indicator of healthy BG regulation. Being obese or overweight, or in general, a higher body mass index (BMI) has been linked to having a higher risk of developing diabetes [10] in the previous studies. Blood glucose forecasting is an active area of research that has been addressed with different machine learning and deep learning approaches including ensemble methods, attention methods, and knowledge distillation [11]–[13]. However, to the best of our knowledge, the use of diet, physical activity, work routine, and previous baseline glucose parameters to predict the area under the glucose curve remains unexplored. Despite the increasing interest in the area under the glucose curve as a metric to estimate the risk of hyperglycemia [14], [15], an in-depth ML-based analysis is yet to be published.

In this paper, we aim to address quantified relationships of diet, physical activity, and work routine with hyperglycemia. Moreover, we propose a machine learning solution for estimating the postprandial AUC based on easily available information such as CGM readings, diet, work routine, and wearable sensor data. To summarize, our contributions are as follows: (i) formulating a problem of predicting PAUC in advance based on diet, work habit, and physical activity, (ii) designing a system with wearables and log-keeping to solve the problem, (iii) conducting a user study to collect the required data, and (iv) implementing GlucoLens for PAUC and hyperglycemia prediction and diverse counterfactual (CF) explanations.

II. MATERIALS AND METHODS

A. System Overview

To investigate the questions about the relationships of diet and activity with postprandial BG, we designed a system of four data sources: a wearable device with motion sensors, a CGM device, food logs, and work logs. As this study was not only about prediction but also about interpretability, the system's data processing tool had to be able to process the raw data and convert them to compatible electronic formats, which would also be human-readable. The processed data would then be used to train ML models which are capable of making accurate predictions about the PAUC given the type of diet and activity. The system is illustrated in Fig. 2.

Suppose, for a specific day i, we have food logs $X_{food}^{(i)}$, work logs $X_{work}^{(i)}$, wearable data $X_{wearabele}^{(i)}$, and CGM readings $X_{CGM}^{(i)}$, then our goal is to learn the function f_y so that it reads the logs and provides the estimated outcome, $\hat{y}$, which is very close to the actual outcome, y.

$$\hat{y} = f_y(X_{food}^{(i)}, X_{work}^{(i)}, X_{CGM}^{(i)}, X_{wearabele}^{(i)})$$

B. User Study

To develop the proposed system, we conducted a user study by recruiting full-time working individuals living in a U.S. city. Appropriate IRB approval and informed consent were obtained before the data collection. Each participant was given a CGM device and an activPAL wearable [16] device. Lunch was delivered at work from select restaurants
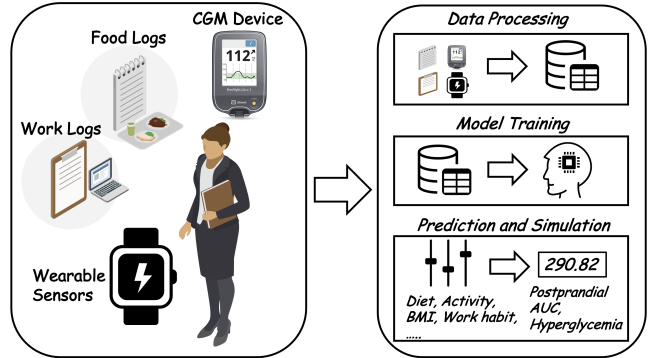

Fig. 2: The GlucoLense system's body sensor network is composed of food logs, work logs, a CGM device, and a wearable sensor. Data from all these sources are combined to create a unified dataset to train a model.

on every working day and each participant received printed forms to maintain the food logs and work logs. The option of homemade meals was not considered for lunch on working days because it would make the task of estimating the macronutrients difficult. On the other hand, the selected restaurants already had the macronutrients for all their items available online, so it was comparatively easier to estimate the nutritional components for every meal consumed.

In the food logs, the participants noted down the time and what they ate in every meal including if there were any leftovers. The participants also logged the amount of water and any supplements (e.g., multivitamins) they were taking every day. In the work logs, they noted when they started working, when they stopped working, how they arrived at work or if they were working from home, and approximately what percentage of working time they spent sitting, standing, and walking.

The data collection ran in three different periods: a 1-week baseline period, a 2-week intervention period named 'Condition 1', and a 2-week intervention period named 'Condition 2'. The baseline week did not have any intervention but the participants wore their CGM devices and activPAL. Two interventions were 'recommending to be standing' and 'recommending to be moving' as much as possible during work. All participants were provided with both of the interventions, but the temporal order was random. Therefore, for some participants, the temporal order was the baseline, stand, move, and for the other participants, it was the baseline, move, stand. In this study, we have included our analysis based on the data of 10 participants having an average baseline BMI of 32.8 ± 4.5.

The activPAL sensor records an event whenever the user's activity changes. The different activities or events detected by the device are: sedentary, standing, stepping, cycling, primary lying, secondary lying, and seated transport. For each event, the event start time and the duration of the event are recorded. The CGM device reported the blood glucose level averaged over every 15-minute window.

C. Data Processing

In this study, one of the main interests was predicting postprandial blood glucose during work days and investigating how diet and activity during work days affect postprandial AUC. Moreover, the participants were provided standardized lunch on the working days, whereas they ate anything they liked on the weekends. In the food logs, the participants kept track of any leftover portions which allowed us to accurately extract the amount of calories and macronutrients consumed during lunch. The food logs were maintained as handwritten logs. They were processed through Google Cloud Vision OCR to create electronic logs followed by some human intervention for issues that could not be resolved by the OCR. The amounts of macronutrients consumed were used to estimate glycemic loads (*GLs*) using the formula from [17].

$$GL = 19.27 + (0.39 \times \text{net carb.}) - (0.21 \times \text{fat})$$
$$- (0.01 \times \text{protein}^2) - (0.01 \times \text{fiber}^2) \quad (1)$$

The work logs were also handwritten and they were processed manually to convert them to electronic format. From activPAL sensors data and with the help of work logs, the durations of sitting, standing, and stepping were calculated for the day to lunch, as well as the durations of sitting, standing, and stepping during work hours for the day until lunch. For this work, fasting glucose was defined as the minimum CGM reading between 6 AM and 10 AM. The recent CGM was defined as the average CGM reading of the same prediction day from midnight to 8 AM. A complete list of the input features of the 'Sensor+Macro' feature set can be found in Fig. 3. Two additional inputs are used in the 'All' feature set: an activity score calculated from self-reported activity logs during work and the glycemic load. In the 'Self+Macro' feature set, the 6 features containing sitting, standing, and stepping durations are replaced by the activity score based on self-reported activity logs. The activity score was calculated from the self-reported activities in the work logs. In the work logs, each user reported the percentage of their working hours spent sitting, standing, and walking. As mentioned in Section II-B, there were three phases: Baseline, Condition 1, and Condition 2. The recent activity score is calculated by taking the average percentage of time spent in walking activity in the previous days of the same phase and adding with $\frac{1}{2} \times$ the average percentage of time spent in standing activity in the previous days of the same phase. In the 'Self+GL' and 'Sensor+GL' feature sets, the macronutrients: net carbs, fat, protein, and fiber are removed and replaced with the glycemic load calculated in Equation 1. The relationship of all five different feature sets can be found in Fig. 3.

TABLE I: Size of the dataset depending on the feature set chosen. The meanings of the different feature sets are explained in Fig. 3.

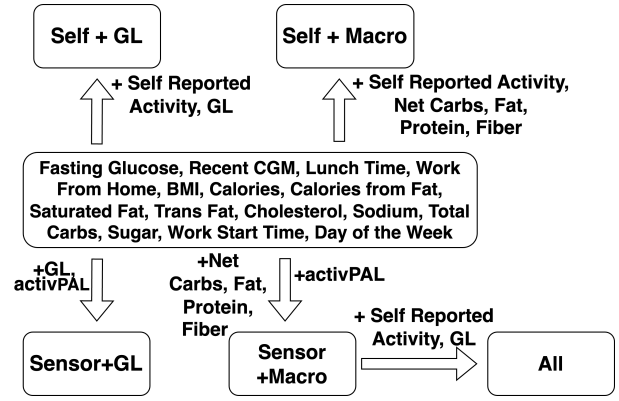| Feature set	Sensor +Macro	Self +Macro	Sensor +GL	Self +GL	All
Train size	127	140	127	140	127
Test size	32	35	32	35	32

Fig. 3: A comparison of the five different feature sets used in this study. GL = glycemic load of the meal. Self = activity scores calculated by self-reported activity duration in work logs. Macro = macronutrients that are used to calculate glycemic load: net carb, fat, protein, and carb. Sensor = activity metrics from activPAL sensor: duration of sitting, standing, and stepping activities of the day before lunch and the same metrics from the start of working to just before lunch of the same day.

D. ML Models

Three regression models, Random Forest (RF), Ridge Regressor, and MLP Regressor were trained for each of the three tasks: estimating PAUC, ∆PAUC, and MaxPBG. MLPs and Random Forests are capable of making effective predictions with proper feature extractions [18], [19], whereas linear regression methods with regularization, such as Ridge Regression [20] and Lasso Regression [21] are popular choices as baselines. Neural networks are usually data-hungry, which is why, on small datasets, classical ML methods can show competitive and even better performance than neural networks.

Three variations of RF, three variations of Ridge, and thirteen variations of MLP were trained and tested. Therefore, in total 19 models, 3 tasks each, 5 feature sets each, and 3 random seeds were used. The variations of RF, Ridge, and MLP can be found in Table II and Table III. For each experiment, 20% data instances were assigned to the test set, and 80% data instances were assigned to the training set. The exact number of instances for training and test sets are represented in Table I.

E. Hyperglycemia Detection and Counterfactual Explanations

GlucoLens was also trained for hyperglycemia detection with RF backbone models. Both MLP and RF models were trained for hyperglycemia detection and RF (avg accuracy 74%) outperformed MLP (best accuracy 71%). Counterfactual explanations can provide insights on features responsible for an undesired health outcome and possible remedies to overcome them [22], [23]. As a primary goal of the paper was to explore more knowledge about the reasons for and ways to prevent hyperglycemia, a DiCE-based counterfactual expla-

nations generator is integrated with GlucoLens. GlucoLens provides multiple counterfactual explanations that are diverse and achievable with small perturbations from the original example [24].

TABLE II: An overview of all experiments conducted for the regression problem. MLP = multilayer perception. RF = random forest. Ridge = ridge regression. n_{est} = number of estimators in random forest. Meanings of the outcomes PAUC, ΔPAUC, and MaxPBG can be found in Fig. 1.

Target outcomes	PAUC, ΔPAUC, MaxPBG
Feature sets	Sensor + Macro, Self + Macro, Sensor + GL, Self + GL, All
Models	RF, Ridge, MLP
Ridge variations	$\alpha \in \{1, 0.1, 0.01\}$
RF variations	$n_{est} \in \{10, 50, 100\}$
MLP variations	13 variations; see Table III
Random seeds	3 different seeds
Total # experiments	$3 \times 5 \times (3 + 3 + 13) \times 3 = 855$

TABLE III: Variations of the multilayer perceptron (MLP regressor). Different variations have been tested by varying the depth and size of each layer.

Variation no.	# Hidden layers	Sizes of hidden layers
1	3	(20, 10, 5)
2	4	(40, 20, 10, 5)
3	4	(60, 30, 15, 7)
4	5	(80, 40, 20, 10, 5)
5	5	(100, 50, 25, 12, 6)
6	5	(120, 60, 30, 15, 7)
7	5	(140, 70, 35, 17, 8)
8	5	(160, 80, 40, 20, 10)
9	8	(80, 40, 20, 20, 20, 20, 10, 5)
10	8	(100, 50, 25, 25, 25, 25, 12, 6)
11	8	(120, 60, 30, 30, 30, 30, 15, 7)
12	8	(140, 70, 35, 35, 35, 35, 17, 8)
13	8	(160, 80, 40, 40, 40, 40, 20, 10)

III. RESULTS

A. Best Combination for Each Outcome

Three different outcomes were chosen for the regression problem: i) PAUC, ii) ΔPAUC, and iii) MaxPBG. In Table IV, we see that for PAUC, ΔPAUC, and MaxPBG, the best NRMSE values are 0.123, 0.622, and 0.132 respectively. RF predictors obtained all three best results. Although 13 different variations were tested for MLPs, none of them achieved the best performance on any of the three tasks.

TABLE IV: Summary of the best results for each target outcome. Three different models were tested with five different combinations. Meanings of the outcomes PAUC, ΔPAUC, and MaxPBG can be found in Fig. 1. RF = random forest. NRMSE = normalized root mean squared error.

Target outcome	Best feature set	Best model	Best hyperparameters	Test RMSE	Test NRMSE
PAUC	All	RF	$n_{est} = 10$	39.2	0.123
ΔPAUC	Self + Macro	RF	$n_{est} = 100$	58.8	0.622
MaxPBG	All	RF	$n_{est} = 100$	16.4	0.132

B. Effect of Feature Sets

The impact of different input features and their combinations is described in Table V. All features and Sensor + Macro result in the best NRMSE scores (0.123 and 0.132) across all feature sets for estimating PAUC and MaxPBG, while the best NRMSE (0.622) for ΔPAUC estimation comes from the Self + Macro feature set. The average NRMSE across all five feature sets are 0.130, 0.736, and 0.144 for PAUC, ΔPAUC, and MaxPBG estimation, respectively.

TABLE V: Effect of feature set on the regression tasks. The corresponding hyperparameters of the random forest (RF) and Ridge regression models are presented in parentheses. NRMSE = normalized root mean squared error.

Feature set	PAUC NRMSE	ΔPAUC NRMSE	MaxPBG NRMSE	Model for PAUC	Model for ΔPAUC	Model MaxPBG
Sensor + Macro	**0.123**	0.798	**0.132**	RF (50)	RF (100)	RF (100)
Self + Macro	0.139	**0.622**	0.161	RF (10)	RF (100)	Ridge (0.01)
Sensor + GL	0.125	0.827	0.134	RF (100)	RF (100)	RF (100)
Self + GL	0.139	0.626	0.159	Ridge (0.01)	RF (50)	Ridge (0.01)
All	**0.123**	0.806	**0.132**	RF (10)	RF (100)	RF (100)
Average	0.130	0.736	0.144	-	-	-

C. Performance of MLP

Out of the 13 different variations of MLP regressors, none of them were the best for any of the three outcomes or any of the 15 outcome-feature_set combinations, as shown in Table IV and Table V. It encouraged us to look deeper into the results of the MLP variations. We present the best performances by each of the 13 MLP variants for each of the three outcomes in Table VI. MLP variation no. 13 is the largest of all the MLP variations used in our experiments and it performed better than any other MLPs in all three tasks. It raises the question of whether even larger and deeper models would be more accurate and potentially better than the RF and Ridge models. We wish to investigate this in future work.

TABLE VI: Percentage of error in terms of NRMSE (i.e. NRMSE $\times$ 100) for different variations of MLP in three different regression tasks. Results are rounded to the nearest integer unless any other result rounds to the same integer as the best result. The details of the MLP variations can be found in Table III. For the best results of PAUC, ΔPAUC, and MaxBPG, the corresponding feature sets are Sensor + GL, Self + Macro, and Sensor + GL.

Variation	1	2	3	4	5	6	7	8	9	10	11	12	13
PAUC	74	29	27	22	21	19	18	18	19	18	18	18	**17**
ΔPAUC	89	82	81	81	80	80	81	79	80	79	79	80	**78**
MaxPBG	50	24	24	21	21	19	18.3	18.0	19	18	19	19	**17.5**

D. Prediction with XGBoost and TabNet

One may wonder if there are other machine learning models or neural networks that could be used to evaluate the system's efficacy. We believe that advanced neural networks integrated with our system will be able to perform more accurate results but it will require more data to train them. To explore more, apart from the random forest, MLP, and ridge regressions, we also trained two comparatively more advanced ML models: XGBoost [25] and Tabnet [26]. In our experiments, Random Forest outperformed both TabNet and XGBoost in estimating PAUC. TabNet trained with 100
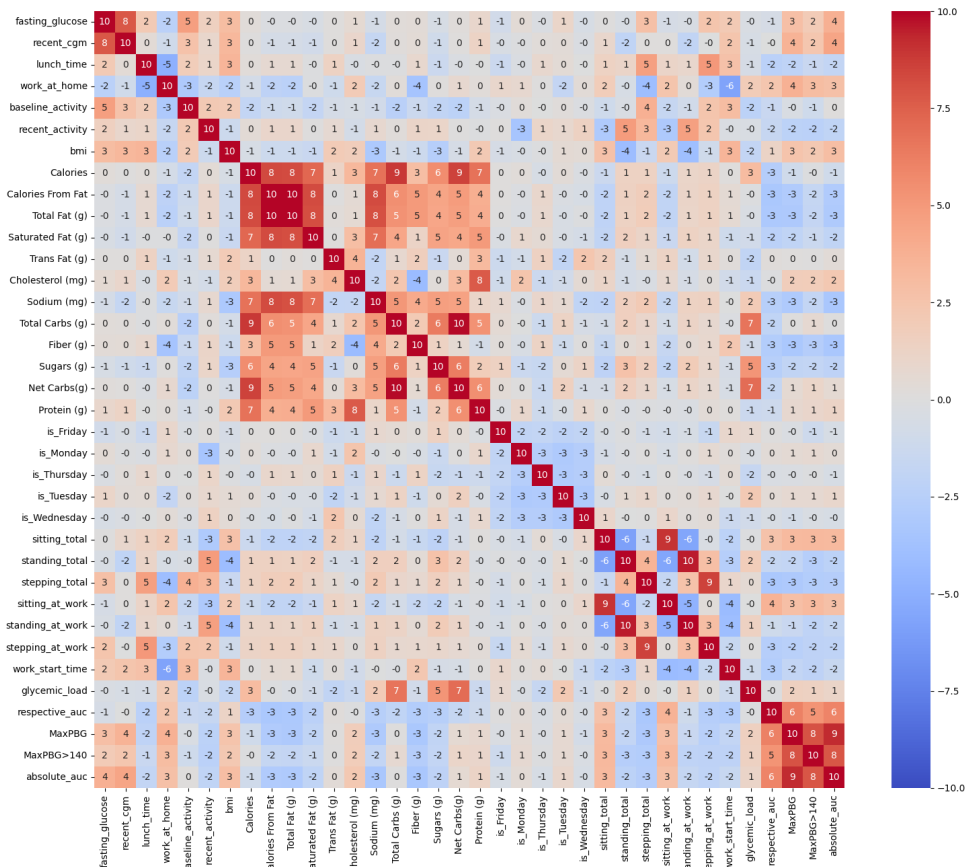
Fig. 4: Overall Pearson correlation matrix with the coefficients multiplied by 10 to avoid printing decimal points in the figure. The amount of fiber, duration of time in stepping, and total fat intake are some of the features working in favor of lowering postprandial area under the curve (PAUC) and related outcomes. PAUC is represented as 'absolute_auc' in this figure and increase in PAUC after lunch, ΔPAUC as 'respective_auc'. On the other hand, duration spent sitting, higher fasting glucose, a higher BMI, and working at home are some of the features positively correlated with PAUC.

epochs provided an NRMSE of 0.147 and XGBoost provided an NRMSE of 0.137. A summary of the performance of XGBoost and TabNet for different feature sets is presented in Table VII.

TABLE VII: Test set normalized root mean squared errors (NRMSE) of the XGBoost and TabNet models for different feature sets for estimating the postprandial area under the curve (PAUC).

Feature set	TabNet	XGBoost
Sensor + GL	0.160	**0.137**
Sensor + Macro	**0.147**	0.139
Self + GL	0.154	0.152
Self + Macro	0.151	0.149
All	0.151	**0.137**

E. Correlation Analysis

In addition to the results of the prediction problems, we also present Pearson correlations of the factors with the outcome variable PUAC in Fig. 4. As it is recommended to keep MaxPBG below 140 mg/dL for non-diabetic people [27], a binary outcome of MaxPBG > 140 was added to the correlation analysis to find out what features are positively or negatively correlated with this outcome. The observed correlations of this outcome with the input features were similar to the correlations of the other three outcomes.

We notice a positive correlation between the negative outcomes (high PAUC or high MaxPBG) and the features: BMI, sitting duration, and working at home. We also notice that overall, a delayed lunch is correlated with a lower AUC. Finally, fiber is negatively correlated with the outcomes as expected. This correlation analysis also shows us the risk of postprandial hyperglycemia because of higher PAUC or ΔPAUC metrics. If we look at Fig. 4, especially the row of 'MaxPBG > 140', which directly represents the risk of hyperglycemia, we notice that it has a very high correlation coefficient with both 'abosolute_auc' (PAUC) and

'respective_auc' (ΔPAUC), with values 8 and 5 respectively (on a scale of -10 to 10). It indicates that a higher PAUC or ΔPAUC may lead a person to develop hyperglycemia in the long run.

F. Results of Hyperglycemia Detection and Diverse Counterfactual Explanations

GlucoLens achieves an accuracy of 74% and an F1 score of 0.55 in hyperglycemia detection with a small training dataset. The visualization of counterfactual explanations in Fig. 5 highlights insights for avoiding hyperglycemia by examining the influence of various features on postprandial blood glucose outcomes. The original data point of Fig. 5a associated with hyperglycemia (Outcome=1) is represented by a solid blue line with a blue dot, while three counterfactual scenarios are depicted using dashed lines. Counterfactual 1 (orange, Outcome=0) illustrates a scenario where increasing fiber intake changes the outcome. In Counterfactual 2 (green, Outcome=0), increasing fiber by a large amount, despite additional cholesterol intake, changes the class label. Counterfactual 3 (red, Outcome=0) does not make any change in diet but increases physical activity (stepping duration) significantly to change the outcome.

Similarly, in the second example with a normal outcome (Outcome=0) as shown in Fig. 5b, counterfactual scenarios reveal potential pathways to hyperglycemia. Counterfactual 1 (orange, Outcome=1) highlights how an increase in sedentary time at work (in seconds) and an early work start time can increase the chance of hyperglycemia. In Counterfactual 2 (green, Outcome=1) and Counterfactual 3 (red, Outcome=1) a higher starting fasting glucose and recent CGM readings in addition to much longer sedentary duration contributed to the class label to flip from normal to hyperglycemia. These findings highlight the importance of diet, activity, and habits in managing glucose levels, demonstrating the value of counterfactual explanations for personalized recommendations.

IV. DISCUSSION

A. Summary of the Results

We have presented an important problem of estimating the postprandial area under the curve (PAUC), change in PAUC (ΔPAUC), and maximum postprandial blood glucose level (MaxPBG). Based on our experiments, we found that random forest (RF) models outperform multilayer perceptions (MLP) and ridge regression models as shown in Table V. We also chose our features from five different feature sets as illustrated in Fig. 3. Although our feature sets use 31 features as input to the model when choosing the set of 'All' features, all these features are derived from only four sources of data, which makes it easier to have the required data easily available when needed for the model.

B. Different Interpretation of the Results

Our best-found NRMSE of 0.123 implies that the predicted PAUC value was on average within a 12.3% error margin from the actual values of PAUC. To interpret the performance in another way, we also explored the percentage of test cases
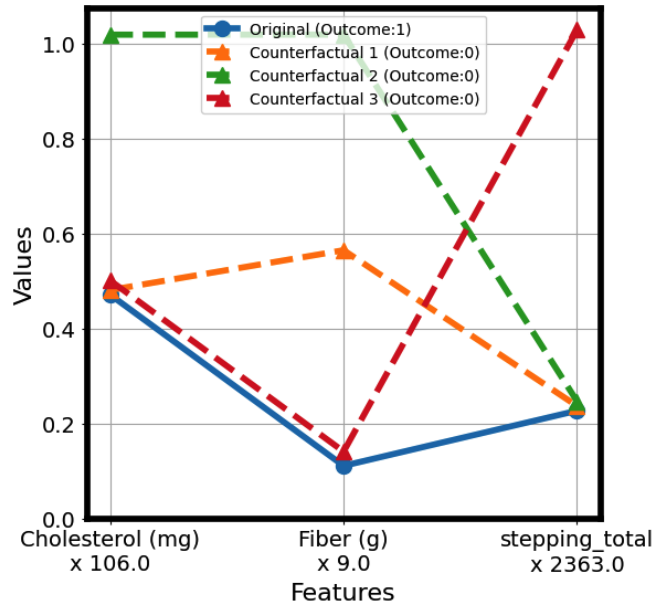
(a) Original label: Hyperglycemia, CF label: Normal
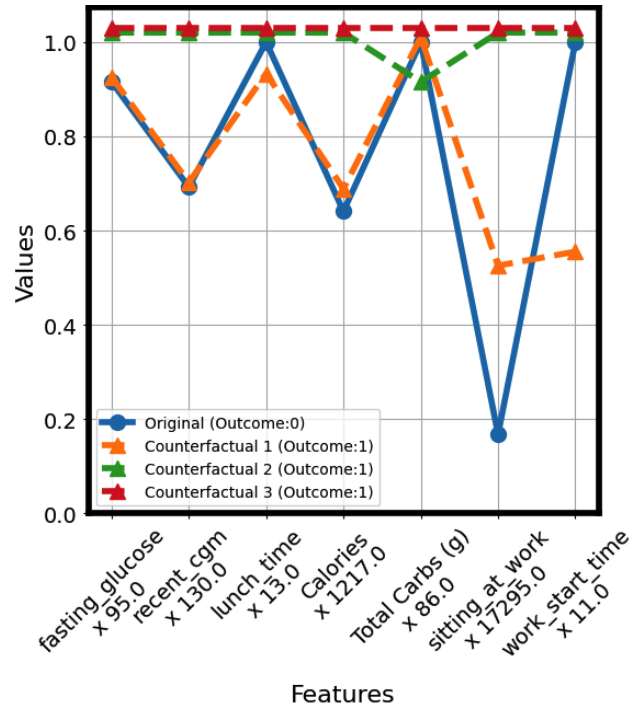
(b) Original label: Normal, CF label: Hyperglycemia

Fig. 5: Counterfactual explanations for a normal and a postprandial hyperglycemic event. Features not presented in the figures had the same value in the original and all its counterfactual examples. Feature values of the counterfactual examples were plotted with small shifts (+0.01 for CF1, +0.02 for CF2, +0.03 for CF3) for better visualization. Units not shown in the figure: stepping_total (s), sitting_at_work (s), fasting_glucose (mg/dL), recent_cgm (mg/dL), lunch_time (h), work_start_time (h). Plotted values are scaled. Multiply by the given factors to obtain actual values.

falling within an error tolerance. From the actual PAUC values and the predicted PAUC values, the ratio of test cases within 5%, 10%, 15%, and 20% errors were calculated. Among the predictions made by our system, we have verified that 33% of the cases had an error of less than 5%, 61% of the cases had an error of less than 10%, 81% of cases had an error of less than 15%, and 93% cases had an error less than 20%. Thus only 19% of the cases had an error more than 15% and only 7% cases had an error over 20%. We believe that with more training data, our system will be able to predict most of the cases within a very small margin of error. The percentage of test cases within 5%, 10%, 15%, and 20% error margins for the XGBoost model were 30%, 55%, 78%, and 92% respectively, all lower than our random forest model. Therefore, our random forest model outperforms XGBoost in this metric as well.

C. Alternative Feature Search Methods

Another dimension to explore could be to find possible feature sets other than the five options presented in Fig. 3. One way could be to perform an exhaustive search within the features. The problem with that approach would be the computational cost. As we have 31 features, we would have 2^{31} possibilities which would be infeasible to explore. However, we have done an additional experiment to find effective feature subsets. Among all the models, our random forest (RF) was the best model so far with an NRMSE of 0.123. We limited the number of features by restricting the number of leaf nodes in RF models to 24, 48, and 96. The 48-leaf-node limit outperformed the others, achieving an NRMSE of 0.121, surpassing our previous best result of 0.123. This approach offers a more rational feature selection method, as limiting leaf nodes helps identify features with higher information gains, reduces overfitting, and improves generalization.

V. CONCLUSION

In this study, we have analyzed different diet and physical activity features to develop an interpretable ML system for estimating postprandial blood glucose parameters. We believe that our tools will be helpful to people diagnosed with or at risk of diabetes to better regulate their condition and avoid unwanted outcomes. Based on the experiments with different variations of models and feature sets, our GlucoLens system with Random Forest-based backbone outperforms the baseline models by a margin of 12 to 21%. Additionally, with the help of correlation analysis, we established the relationship between PAUC and the risk of hyperglycemia, as well as the features leading to an increase or decrease in the risk of hyperglycemia.

Our proposed GlucoLens system achieves a 74% accuracy on hyperglycemia prediction. Moreover, it recommends different interventions to avoid hyperglycemia based using diverse counterfactual explanations. Based on the explanations, we showed that a regulated diet and higher physical activity can avoid hyperglycemia.

REFERENCES

[1] R. R. Gehlaut, G. Y. Dogbey, F. L. Schwartz, C. R. Marling, and J. H. Shubrook, "Hypoglycemia in type 2 diabetes-more common than you think: a continuous glucose monitoring study," *Journal of diabetes science and technology*, vol. 9, no. 5, pp. 999–1005, 2015.

[2] G. E. Crichton and A. Alkerwi, "Physical activity, sedentary behavior time and lipid levels in the observation of cardiovascular risk factors in luxembourg study," *Lipids in health and disease*, vol. 14, pp. 1–9, 2015.

[3] M. Mouri and M. Badireddy, "Hyperglycemia," in *StatPearls [Internet]*. StatPearls Publishing, 2023.

[4] S. Alvarez, R. Coffey, and A. M. Algotar, "Prediabetes," 2017.

[5] M. R. Castro, *Mayo Clinic: The Essential Diabetes Book 3rd Edition: How to prevent, manage and live well with diabetes*. Simon and Schuster, 2022.

[6] CDC, "National Diabetes Statistics Report — cdc.gov," https://www.cdc.gov/diabetes/php/data-research/index.html, [Accessed June 2024].

[7] "FDA Clears First Over-the-Counter Continuous Glucose Monitor — fda.gov," https://www.fda.gov/news-events/press-announcements/fda-clears-first-over-counter-continuous-glucose-monitor, [Accessed 10-02-2025].

[8] J. B. Echouffo-Tcheugui, L. Perreault, L. Ji, and S. Dagogo-Jack, "Diagnosis and management of prediabetes: a review," *Jama*, vol. 329, no. 14, pp. 1206–1216, 2023.

[9] N. Chakarova, R. Dimova, G. Grozeva, and T. Tankova, "Assessment of glucose variability in subjects with prediabetes," *Diabetes research and clinical practice*, vol. 151, pp. 56–64, 2019.

[10] C. A. Maggio and F. X. Pi-Sunyer, "Obesity and type 2 diabetes," *Endocrinology and Metabolism Clinics*, vol. 32, no. 4, pp. 805–822, 2003.

[11] Y. Han, D.-Y. Kim, J. Woo, and J. Kim, "Glu-ensemble: An ensemble deep learning framework for blood glucose forecasting in type 2 diabetes patients," *Heliyon*, vol. 10, no. 8, 2024.

[12] E. Farahmand, S. B. Soumma, N. T. Chatrudi, and H. Ghasemzadeh, "Hybrid attention model using feature decomposition and knowledge distillation for glucose forecasting," *arXiv preprint arXiv:2411.10703*, 2024.

[13] E. Farahmand, R. R. Azghan, N. T. Chatrudi, E. Kim, G. K. Gudur, E. Thomaz, G. Pedrielli, P. Turaga, and H. Ghasemzadeh, "Attengluco: Multimodal transformer-based blood glucose forecasting on ai-readi dataset," *arXiv preprint arXiv:2502.09919*, 2025.

[14] M. Uemura, Y. Yano, T. Suzuki, T. Yasuma, T. Sato, A. Morimoto, S. Hosoya, C. Suminaka, H. Nakajima, E. C. Gabazza *et al.*, "Comparison of glucose area under the curve measured using minimally invasive interstitial fluid extraction technology with continuous glucose monitoring system in diabetic patients," *Diabetes & Metabolism Journal*, vol. 41, no. 4, pp. 265–274, 2017.

[15] S. Ugi, H. Maegawa, K. Morino, Y. Nishio, T. Sato, S. Okada, Y. Kikkawa, T. Watanabe, H. Nakajima, and A. Kashiwagi, "Evaluation of a novel glucose area under the curve (auc) monitoring system: comparison with the auc by continuous glucose monitoring," *Diabetes & metabolism journal*, vol. 40, no. 4, pp. 326–333, 2016.

[16] K. Lyden, S. K. Keadle, J. Staudenmayer, and P. S. Freedson, "The activpal™ accurately classifies activity intensity categories in healthy adults," *Medicine and science in sports and exercise*, vol. 49, no. 5, p. 1022, 2017.

[17] H. Lee, M. Um, K. Nam, S.-J. Chung, and Y. Park, "Development of a prediction model to estimate the glycemic load of ready-to-eat meals," *Foods*, vol. 10, no. 11, p. 2626, 2021.

[18] R. R. Azghan, N. C. Glodosky, R. K. Sah, C. Cuttler, R. McLaughlin, M. J. Cleveland, and H. Ghasemzadeh, "Cudle: Learning under label scarcity to detect cannabis use in uncontrolled environments using wearables," *IEEE Sensors Journal*, 2025.

[19] A. Mamun, C.-C. Kuo, D. W. Britt, L. D. Devoe, M. I. Evans, H. Ghasemzadeh, and J. Klein-Seetharaman, "Neonatal risk modeling and prediction," in *2023 IEEE 19th International Conference on Body Sensor Networks (BSN)*. IEEE, 2023, pp. 1–4.

[20] G. C. McDonald, "Ridge regression," *Wiley Interdisciplinary Reviews: Computational Statistics*, vol. 1, no. 1, pp. 93–100, 2009.

[21] J. Ranstam and J. A. Cook, "Lasso regression," *Journal of British Surgery*, vol. 105, no. 10, pp. 1348–1348, 2018.

[22] A. Mamun, L. D. Devoe, M. I. Evans, D. W. Britt, J. Klein-Seetharaman, and H. Ghasemzadeh, "Use of what-if scenarios to help explain artificial intelligence models for neonatal health," *arXiv preprint arXiv:2410.09635*, 2024.

[23] A. Arefeen, S. Khamesian, A. Grando, B. M. Thompson, and H. Ghasemzadeh, "Glyman: Glycemic management using patient-centric counterfactuals," in *IEEE-EMBS International Conference on Biomedical and Health Informatics*.

[24] R. K. Mothilal, A. Sharma, and C. Tan, "Explaining machine learning classifiers through diverse counterfactual explanations," in *Proceedings of the 2020 conference on fairness, accountability, and transparency*, 2020, pp. 607–617.

[25] T. Chen and C. Guestrin, "Xgboost: A scalable tree boosting system," in *Proceedings of the 22nd acm sigkdd international conference on knowledge discovery and data mining*, 2016, pp. 785–794.

[26] S. Ö. Arik and T. Pfister, "Tabnet: Attentive interpretable tabular learning," in *Proceedings of the AAAI conference on artificial intelligence*, vol. 35, no. 8, 2021, pp. 6679–6687.

[27] J. E. Gerich, "Postprandial hyperglycemia and cardiovascular disease," *Endocrine Practice*, vol. 12, pp. 47–51, 2006.